sustainability

MDPI

Article

Influence of Fine Recycled Concrete Powder on the Compressive Strength of Self-Compacting Concrete (SCC) Using Artificial Neural Network

Sara Boudali [1,*], Bahira Abdulsalam [2], Amir Hossein Rafiean [3], Sébastien Poncet [4], Ahmed Soliman [5] and Adel ElSafty [6,*]

1 Mechanical Engineering Department, Faculty of Engineering, Université de Sherbrooke and Groupe ABS, Sherbrooke, QC J1L 2G7, Canada
2 CIISolutions Composites Infrastructure Innovation Solutions Corp., Toronto, ON M4H1L6, Canada; bahira.abdulsalam@compositeinfrastructure.com
3 Department of Soil and Foundation Engineering, Civil Engineering Faculty, Semnan University, Semnan 35196, Iran; a.h.rafiean@semnan.ac.ir
4 Mechanical Engineering Department, Faculty of Engineering, Université de Sherbrooke, Sherbrooke, QC J1K 2R1, Canada; Sebastien.Poncet@USherbrooke.ca
5 Building, Civil, and Environmental Engineering, Concordia University, Montréal, QC H3G 1M8, Canada; ahmed.soliman@concordia.ca
6 School of Engineering, Civil Engineering, University of North Florida, Jacksonville, FL 32224, USA
* Correspondence: sara.boudali@Usherbrooke.ca (S.B.); adel.el-safty@unf.edu (A.E.); Tel.: +1-819-919-0483 (S.B.); +1-904-620-1398 (A.E.)

check for updates

Citation: Boudali, S.; Abdulsalam, B.; Rafiean, A.H.; Poncet, S.; Soliman, A.; ElSafty, A. Influence of Fine Recycled Concrete Powder on the Compressive Strength of Self-Compacting Concrete (SCC) Using Artificial Neural Network. *Sustainability* **2021**, *13*, 3111. https://doi.org/10.3390/su13063111

Academic Editors: Francesco Nocera, Rosa Giuseppina Caponetto, Giada Giuffrida and Maurizio Detommaso

Received: 27 January 2021
Accepted: 2 March 2021
Published: 12 March 2021

Abstract: This paper aims to investigate the effect of fine recycled concrete powder (FRCP) on the strength of self-compacting concrete (SCC). For this purpose, a numerical artificial neural network (ANN) model was developed for strength prediction of SCC incorporating FRCP. At first, 240 experimental data sets were selected from the literature to develop the model. Approximately 60% of the database was used for training, 20% for testing, and the remaining 20% for the validation step. Model inputs included binder content, water/binder ratio, recycled concrete aggregates' (RCA) content, percentage of supplementary cementitious materials (fly ash), amount of FRCP, and curing time. The model provided reliable results with mean square error (MSE) and regression values of 0.01 and 0.97, respectively. Additionally, to further validate the model, four experimental recycled self-compacting concrete (RSCC) samples were tested experimentally, and their properties were used as unseen data to the model. The results showed that the developed model can predict the compressive strength of RSCC with high accuracy.

Keywords: artificial neural network; self-compacting concrete; compressive strength; fine recycled concrete powder; fly ash

1. Introduction

Concrete is the most used material worldwide and its production has drastically increased during the last decades. Over the past years, this situation has been thoroughly noted in the construction section and initiatives have been made to change what is known as conventional practice in many examples, to search for ways to improve the construction materials performance and lower the impacts, and to produce environmentally friendly materials [1,2]. In recent years, some researchers have tried to evaluate the potential of using recycled concrete aggregates (RCA) as a replacement for natural aggregates (NA) in the concrete [3,4]. Self-compacting concrete (SCC), as one of the most significant advances in the concrete industry, exhibits a better performance than that of conventional concrete [5]. This may be attributed to the association of supplementary cementitious materials (SCM) and filler materials that are considered at nuclear sites and to refine the porosity of the cement paste and reduce permeability. In fact, filler materials are commonly used as additives in SCC to enhance strength and long-term properties [6,7]. Recycled aggregates have been successfully used and their performance was extensively investigated by several researchers to develop self-compacting concrete [8–10].

Efforts have been made to develop an efficient numerical or analytical model to predict concrete compressive strength as one of the critical parameters of SCC. In the literature, quite a few linear and nonlinear regression equations for prediction of compressive strength can be found [11,12]. The majority of these soft computing techniques have rarely been used beyond classic problems. Some developed models depended on Feret's law and Bolomey's equation [13], to predict the 28-days cured-compressive strength without accounting for any strength gain beyond 28 days [14,15]. Alternatively, other sophisticated models have applied soft computing techniques such as function optimization or approximation by genetic algorithms [11] or neural networks [12,16,17]. Among these techniques, artificial neural networks (ANN) became quite popular by many researchers to estimate the performance of conventional concrete [16–18], the performance of recycled aggregate concrete [3,17], and the performance of high-performance concrete [19,20]. Also, few studies have been done on self-compacting concrete incorporating recycled aggregates [21–23]. Lee et al. (2009) proposed a new methodology based mainly on an artificial neural network as a predictive tool to optimize the material properties of an optimum concrete mixture [24]. The computational power of ANN comes from its ability to learn straight from examples, find relationships between input and output parameters, and tolerate relatively imprecise or incomplete tasks, and approximate results, and be even less vulnerable to outliers [18,25]. To the best of the authors' knowledge, there is very little research in literature and lack of a model that predicts SCC compressive strength produced with the combination of RCA and FRCP. Simultaneously, Boudali et al. (2016) had experimentally proven the significant role of FRCP while producing sustainable self-compacting concrete. An addition of 40% of fine recycled concrete improves the strength development of SCC and self-compacting sand concrete [26]. The potential of using FRCP in producing sustainable self-compacted concrete has not been addressed enough in the literature. This study aimed at evaluating the feasibility of using the ANN method for the prediction of the compressive behavior of recycled self-compacting concrete (RSCC). The model developed in this study was designed using MATLAB neural network toolbox functions. In addition to the validation of the present model, new experiments were designed to evaluate the accuracy of the designed ANN model by a separate, unseen experimental database. Then, a parametric study was conducted to evaluate the effect of different inputs, with different percentages, on the compressive strength of RSCC.

2. Neural Network Approach

A neural network model was developed for this paper. The model was developed based on the experimental work conducted by the authors. The model incorporated also several experimental results from the literature used for analysis and verification. The following explains the basic principles used to build the ANN model and the details about the experimental data sets.

2.1. Basic Principles

Similar to the biological brain, ANN processes, and information from input data [27], the neural network modeling can classify data, recognize the pattern, find approximation function, generalize, and simulate complex operations. Such an approach is specifically suitable to predict the characteristics of complicated mixtures [28]. The structure of the ANN model could have multiple, parallel layers of nonlinear and linear processing segments, called neurons. These multiple, parallel layers include the input layer, hidden layers, and the output layer. Each layer is comprised of sets of parallel nerves [29].

Experimental data (x_i) is introduced in the input layer. Then, it is adjusted by parameter connection weights (w_{ij}) and biases (b), as weights are the links between neurons and layers. Adjusted inputs go through a summation process for formation of a single input (I_j) (Equation (1)) [30]:

$$I_j = \sum_{i=1}^{n} w_{ij}x_i + b \quad (1)$$

After that, an activation function f(x) is applied to the single input to create an output value of the processing element over hidden layers [30]. The difference between network outputs and satisfied targets represents the error value, which is propagated back to the network through a learning algorithm. This back-propagation network could be considered as the most popular learning/training algorithm since it performs better for predicting multiple targets compared to complex and multilayer networks [28,31]. This algorithm updates the network weights and biases, which allow the model to converge rapidly. Through this training process, ANN synthesizes and memorizes correlations between inputs and outputs. Hence, sufficient and representative data are a must during the training process to permit the network to diagnose the basic structure of the information involved. When the model is well trained, it could have the ability to predict targets for any unseen input set of data within the range of the training data with a satisfying degree of accuracy [29]. Extensive sensitivity studies are performed on various networks using a trial-and-error method to evaluate their performance [32].

2.2. Collected Experimental Data Set

A total of 240 data sets have been collected in the literature from previous experimental works on the compressive strength of RSCC. All collected data were normalized based on the compressive strength results for control specimens made with natural aggregate at the same testing age. In addition, shape correction factors for the collected data were applied to eliminate specimen shape effects on the achieved strength following the Eurocode 2 [33] and recommendations from a previous study [34]. The data sets are presented in Table 1 and Appendix A. These data were divided into three parts for designing the model as follows: training (60%), testing (20%), and validation (20%). This division helped the model to show a good generalization capability [35]. The training set data were used to train the NN models, the entire validation data were used to stop the training process, and all test data were used to assess the performance of the mode after completion of the training process.

Table 1. Statistical characteristics of the experimental database.

	Parameters (Unit)	Min	Max	Mean	Standard Deviation
Inputs	Binder content (B) (kg/m^3)	208	460	363.22	72.33
	Water/binder ratio (W/B)	0.4	0.65	0.49	0.08
	Natural aggregates (NA) (kg/m^3)	0	1290	504.89	454.11
	Recycled concrete aggregates (RCA) (kg/m^3)	0	1215	396.78	398.34
	Natural pozzolana (NP) (kg/m^3)	0	140	7	30.51
	Fly ash (FA) (kg/m^3)	0	185	30.12	61.23
	Fine recycled concrete powder (FRCP) (kg/m^3)	0	140	5.83	27.98
	Natural sand (NS) (kg/m^3)	0	1050	600.03	230.25
	Recycled sand (RS) (kg/m^3)	0	1050	90.1	218.85
	Curing time (days)	3	180	35.04	38.61
Output	Compressive strength of RSCC (MPa)	12	65	37.81	12.22

For making data consistent with the tangent sigmoid transfer function limits in both layers, the data were normalized between −1 and +1 using the following equation (Equation (2)):

$$X_n = \left(1 - (-1)\frac{X - X_{min}}{X_{max} - X_{min}}\right) - 1 \tag{2}$$

where X_{min}, X_{max}, and X_n are the minimum, maximum, and the normalized value of the X data sample, respectively.

2.3. Proposed ANN Model

Ten input parameters were chosen based on their demonstrated effect on the compressive strength, namely, the binder content (B), water/binder (W/B) ratio, natural aggregates (NA), recycled concrete aggregates (RCA), natural pozzolana (NP), fly ash (FA), fine recycled concrete powder (FRCP), natural sand (NS), recycled sand (RS), and time of curing (T). The target parameter was the compressive strength of RSCC at different curing ages.

The appropriate architecture of the proposed ANN model is described in Figure 1. The optimal values of the neural network parameters and the description of input parameters are given in Tables 2 and 3, respectively.

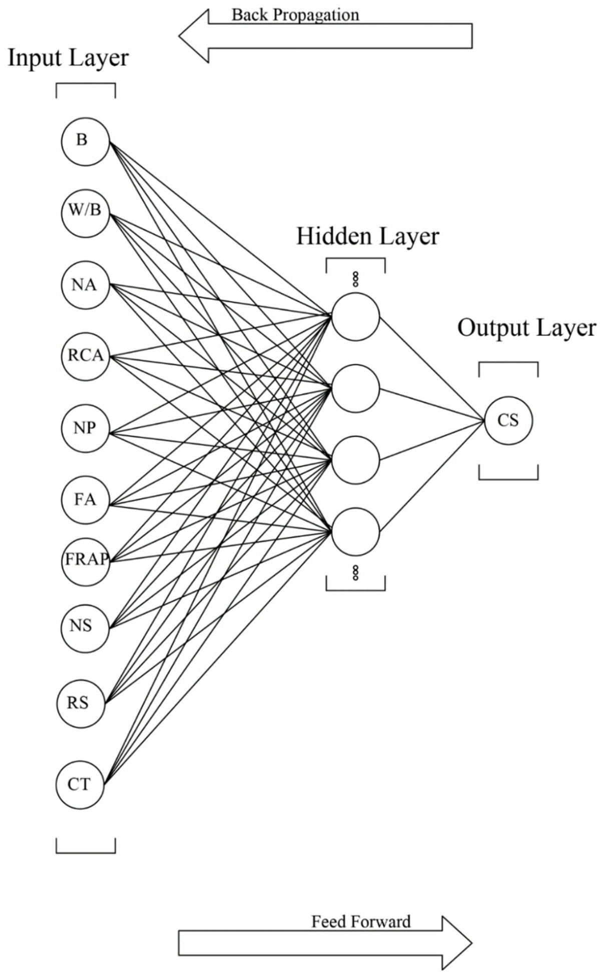

Figure 1. The architecture of artificial neural network model.

Table 2. Values of the neural network parameters used in the ANN model.

Parameters	Values
Number of input layer units	10
Number of hidden layers	1
Number of hidden layer units	10
Number of output layer units	1
Learning rate	0.01
Performance goal	10^{-5}

Table 3. List of the input parameters.

Parameter	Description
B (kg/m^3)	Binder Content
W/B	Water/binder Ratio
NA (kg/m^3)	Natural Aggregate
RCA (kg/m^3)	Recycled Concrete Aggregates
NP (kg/m^3)	Natural Pozzolana
FA (kg/m^3)	Fly Ash
FRCP (kg/m^3)	Fine Recycled Aggregate Powder
NS (kg/m^3)	Natural Sand
RS (kg/m^3)	Recycled Sand
CT (days)	Curing Time

The performance of the best network is evaluated by extensive sensitivity studies performed on various networks using a trial-and-error method. No specific theory has been established for computing the suitable number of neurons in hidden layers and it can be calculated by the following equation (Equation (3)):

$$n = \sqrt{n_i + n_0} + a \tag{3}$$

where n is the number of neurons of the hidden layer, n_i is the number of neurons of the input layer, n0 is the number of the neurons of the output layer, and a is a fixed amount, which ranges between 0 and 10. Based on this formula, the number of neurons of hidden layers ranged from 3 to 13. After so many trials, the highest regression value and the least model error were achieved by 10 neurons. Figure 2 illustrates step by step the flowchart used to select the best ANN model.

The model was designed using MATLAB neural network toolbox functions. For all the networks, the Levenberg–Marquardt algorithm was used to train the network with the log-sigmoid transfer function between the input and hidden layers and the linear transfer function between the second and output layers. This is recognized to be the fastest approach for training networks of moderate size [36].

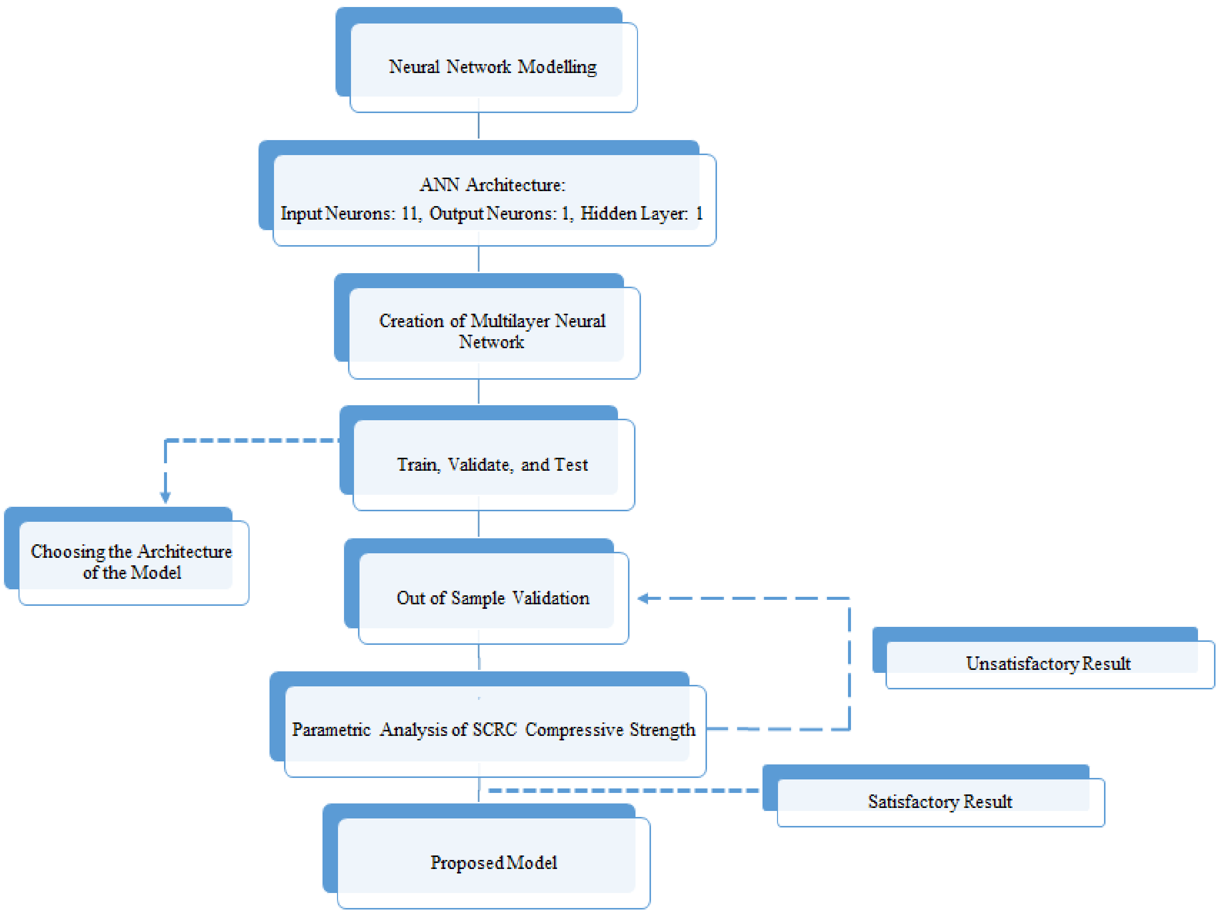

Figure 2. Flow chart used to optimize the neural network model.

3. Results and Discussion

3.1. Model Performance

The performance of any ANN model relies on the success of the training process. A well-designed, trained model should provide accurate output results as prediction, not only for input data used in the training process but also for new experimental data unfamiliar to the designed network within the same range of the training data sets. Additionally, perfect ANN models usually have only slight differences between their validation and testing errors [27]. For this purpose, five essential parameters were chosen to examine the designed model performance and its reliability, including mean square error (MSE), root mean square error (RMSE), mean absolute error (MAE), normalized mean absolute error (NMAE), and linear correlation coefficient (R). Equations (4)–(8) present the formulation for each parameter, and their values are given in Table 4.

$$MSE = \frac{1}{n}\sum_{i=1}^{n}\left(CS_{(model)} - CS_{(actual)}\right)^2 \tag{4}$$

$$RMSE = \sqrt{\frac{1}{n}\sum_{i=1}^{n}\left(CS_{(model)} - CS_{(actual)}\right)^2} \tag{5}$$

$$MAE = \frac{1}{n}\sum_{i=1}^{n}\left|CS_{(model)} - CS_{(actual)}\right| \tag{6}$$

$$NMAE = \frac{\frac{1}{n}\sum_{i=1}^{n}\left|CS_{(model)} - SC_{(actual)}\right|}{CS_{\max(actual)} - CS_{\min(actual)}} \tag{7}$$

$$R^2 = 1 - \frac{\sum_{i=1}^{n}\left(CS_{(actual)} - CS_{(model)}\right)^2}{\sum_{i=1}^{n}\left(CS_{(actual)} - \overline{CS}_{(actual)}\right)^2} \tag{8}$$

where CS_{actual} is the experimental value of compressive strength and CS_{model} is its predicted value by the ANN model.

Table 4. Performance of the designed ANN model.

Evaluation Parameters	R	R^2	MSE	RMSE	MAE	NMAE
Training	0.97	0.93	0.01	0.1	0.043	2.49
Testing	0.96	0.92	0.01	0.1	0.066	4.61

R values greater than 0.8 showed a good connection between the actual and the modeled values [37]. R values for training and testing the ANN model were 0.97 and 0.96, respectively. Figure 3 illustrates the experimental against normalized compressive strength.

Results indicated that the designed ANN model could be a desirable approach for predicting the compressive strength of RSCC. As shown in Figure 4, the experimental and predicted compressive strength values were very close to each other.

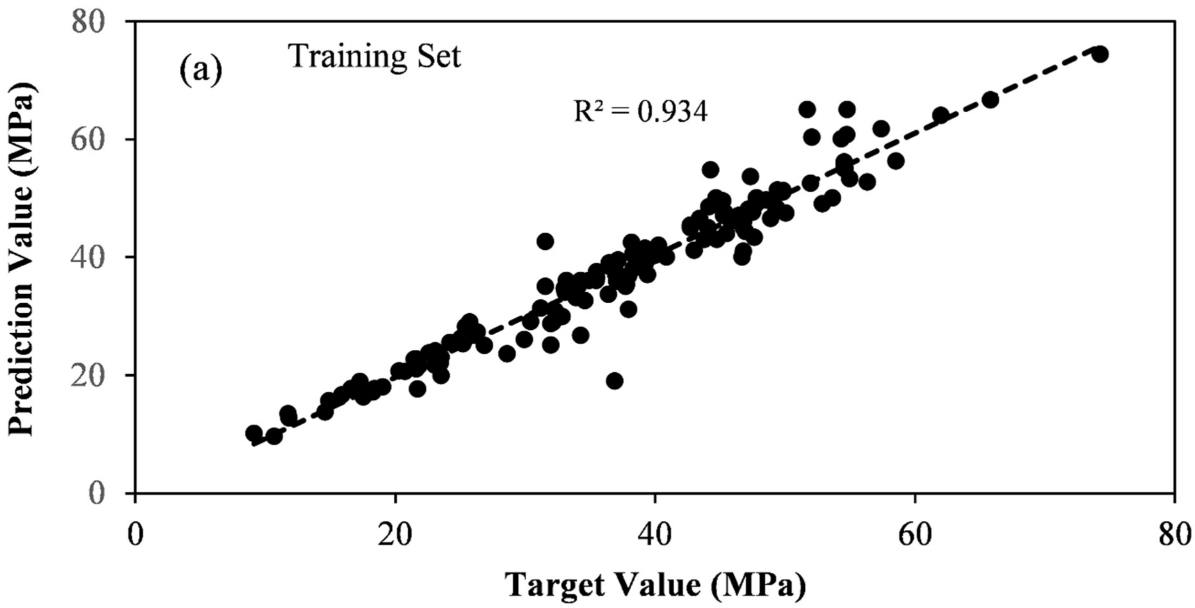

Figure 3. *Cont.*

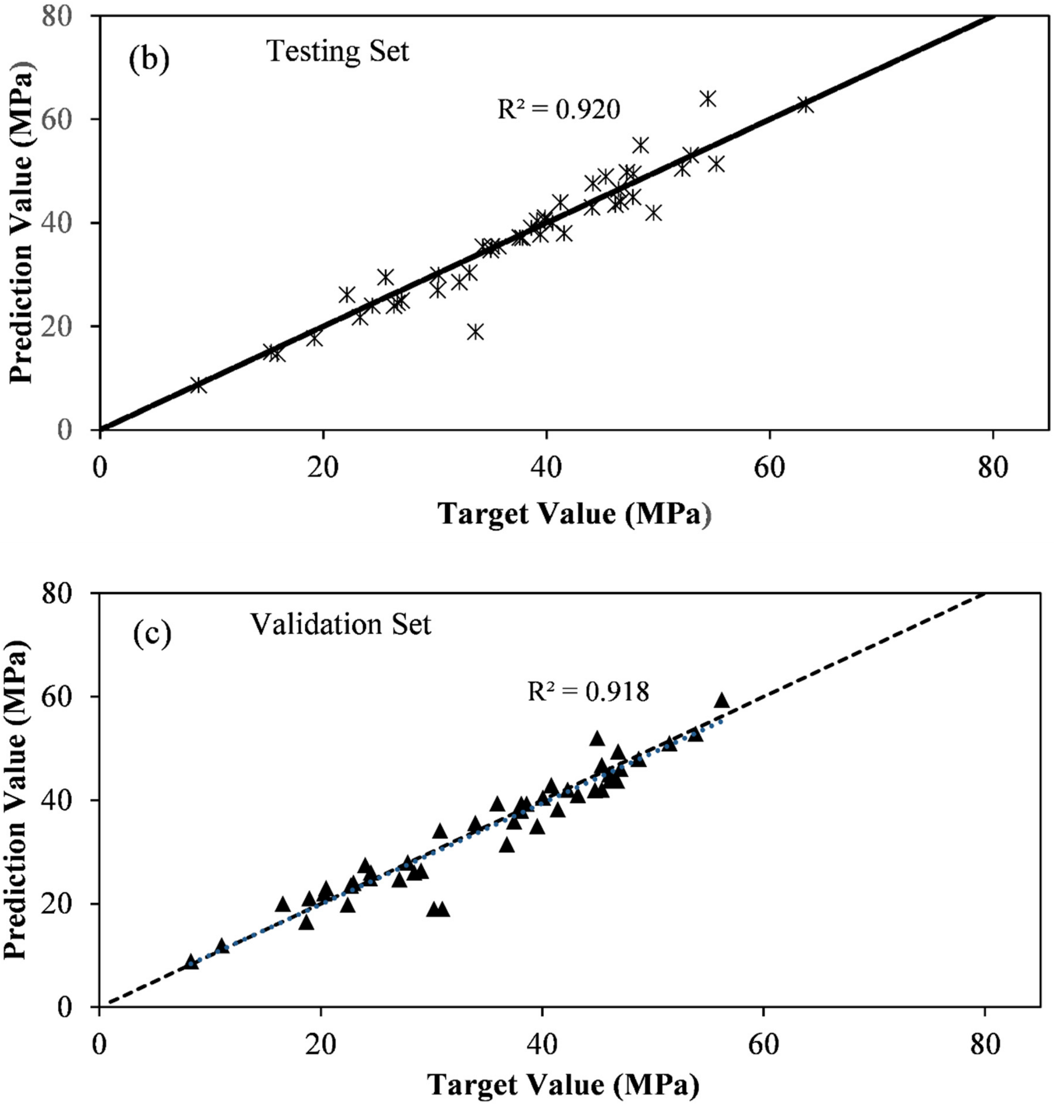

Figure 3. Experimental versus predicted compressive strength values for (**a**) the training set, (**b**) testing set, and (**c**) validation set.

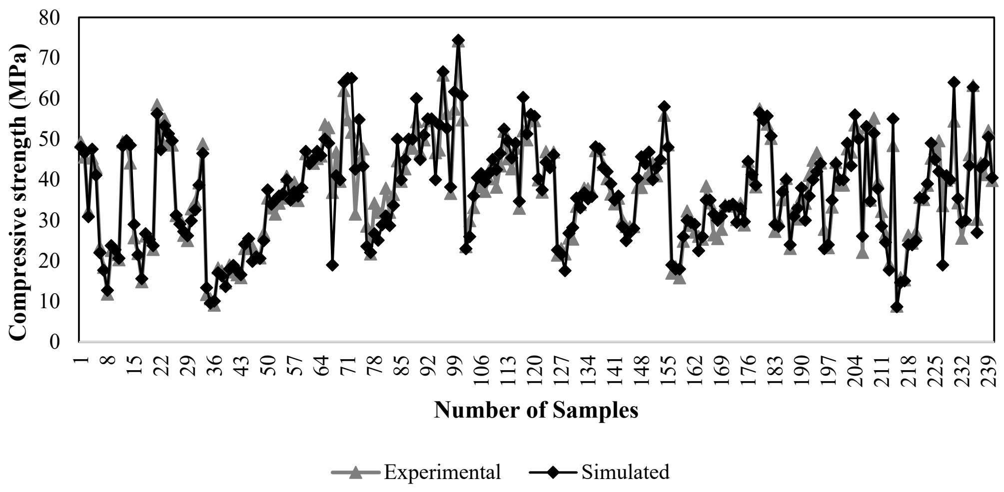

Figure 4. Comparison between the simulated and the experimental results in terms of compressive strength for all samples used in the ANN database.

3.2. Experimental Study for Validation of the Model

To fully validate the developed ANN model, an experimental program was carried out. The completion of this program involved the collection of experimental results on the compressive strength at 7, 28, 60, 90, and 180 days from different mixtures made of recycled concrete at a water-binder ratio of 0.36. Four types of self-compacting sand concrete (SCSC), which is considered as a kind of SCC that contains aggregates with size of less than 5 mm, were prepared by replacing 100% of natural aggregates (NA) and 40% of natural pozzolana (NP) by 100% of recycled aggregates (RA) and 40% fine recycled aggregates powder (FRCP), respectively. The constituent materials of concrete and their proportions were the same for different mixtures. The mixture compositions are given in Table 5.

Table 5. Mix proportions of concrete mixtures for 1 m^3.

Sample				Fine Aggregates (kg/m^3)	Coarse Aggregates (kg/m^3)		Additives	
	Binder (kg/m^3)	W	W/B	S (kg/m^3)	NA(kg/m^3)	RCA (kg/m^3)	FRCP (kg/m^3)	NP (kg/m^3)
SCSC1	620	225	0.36	1213	303	0	0	170
RSCSC2	620	225	0.36	1213	0	303	170	0
RSCSC3	620	225	0.36	1213	303	0	0	170
RSCSC4	620	225	0.36	1213	0	303	170	0

The used materials for the experimental part are described in Boudali et al. [38]. In all mixtures, Portland cement CEMII 42.5 B from local areas in Algeria was used to satisfy the requirements of EN 197 [39]. In terms of additives, natural pozzolana (NP) and fine recycled concrete powder (FRCP) were utilized. The NP was obtained from the deposit of Bouhamidi in the northwest of Algeria, in the Beni-Saf area, and FRCP was extracted by grinding the waste concrete. For superplasticizer, polycarboxylate-based, high-range, water-reducing admixture (HRWR) according to ASTM C494 [40] type F was used as an additive to the composite. The solids' content and specific gravity of the HRWR were 42% and 1.05, respectively. Siliceous sand with a specific gravity of 2.56 and 0.4% of water absorption was considered as a fine aggregate.

Coarse aggregates, either natural or recycled, remained within the size range of 3 to 5 mm. By crushing the construction waste, the used recycled aggregates were extracted in the West Algeria Public Works Laboratory. The compressive strength of recycled aggregates has an average of 40 MPa and had specific gravity and water absorption of 2.54 and 2.5%, respectively. Moreover, the average specific gravity and water absorption of natural aggregates were 2.58 and 1.3%, respectively. Air entraining admixture (AEA) was considered in the order of 35–65 mL/100 kg binder aiming at a fresh air content of 5 $\pm$ 1%. Tap water was utilized throughout the experimental tests.

Mixtures' ingredients were mixed in a mechanical mixer in accordance with ASTM C 192 [41] (Standard Practice for Making and Curing Concrete Test Specimens in the Laboratory). The slump test, according to ASTM C 143, was conducted to evaluate the workability of the fresh concrete. Cube specimens (7 cm $\times$ 7 cm $\times$ 7 cm) were used for each specimen to conduct a compressive strength test. All compressive strength data were normalized based on the compressive strength results for control specimens made with natural aggregate at the same testing age. In addition, shape correction factors for the collected data were applied to eliminate specimen shape effects on the achieved strength following the Eurocode 2 [33] and recommendations from a previous study [34]. Specimens were produced according to NF P 18-400 [42]. The compressive strength of the samples was investigated after 7, 28, 60, 90, and 180 days of curing. Each reported compressive strength value represented the average of three identical samples.

The experimental results were used as unseen inputs to further validate the model (Table 6). The same 10 input parameters including binder content, water/binder ratio, natural aggregate, recycled concrete aggregate, natural pozzolana, fly ash, fine recycled aggregate powder, natural sand, recycled sand, and curing time were given to the developed ANN model and the compressive strength of RSCC as the target predicted by the model. For validating the model, the experimental compressive strengths of RSCC, i.e., the actual ones, were compared to the ones predicted by the model. It showed a good correlation, since the R^2 value between the experimental and predicted compressive strength values was higher than 0.87 (Figure 5).

Table 6. Compressive strength values of mixtures were used as unseen inputs to further validate the model.

	CS (MPa)			
Times (Days)	**SCSC1**	**RSCSC2**	**RSCSC3**	**RSCSC4**
7	24.25	25.22	26.19	27.16
28	38.8	37.83	38.8	45.6
60	43.65	43.65	47.53	53.35
90	45.6	46.56	50.44	54.32
180	47.53	49.5	53.35	55.94

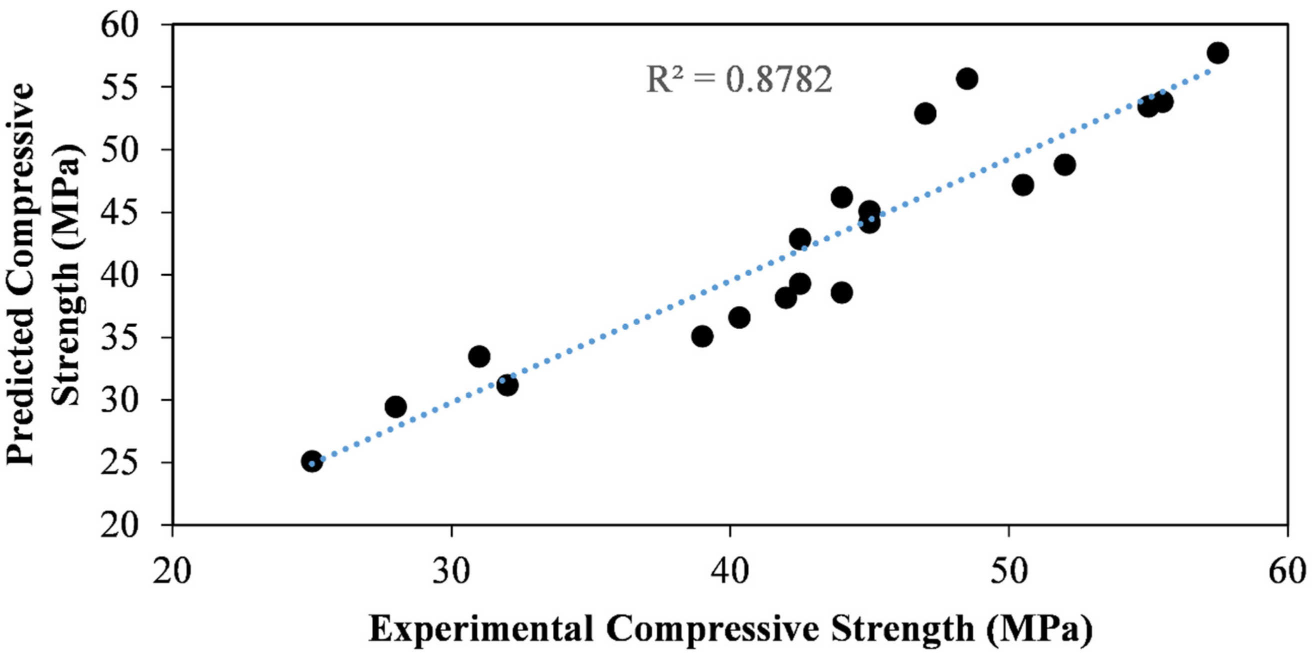

Figure 5. Predicted versus experimental compressive strength results.

3.3. Parametric Analysis

The developed model presented desirable performance and showed its capability for prediction of the compressive strength for different kinds of SCC mixture designs with various sizes of recycled aggregates. This section focuses on utilizing the capabilities of the model in capturing the effect of individual input variables on compressive strength progress. For the analysis, randomly selected concrete mixtures were introduced to the model as new mixtures with different levels within the range of training data of the parameter of interest. Out of the model inputs, the percentage of FRCP, RCA content, and FA were selected to highlight their effects on compressive strength development. Generally, obtained results were in agreement with previous findings by researchers [18], indicating the potential and high capability of the developed ANN model in predicting the performance.

3.3.1. Effect of Recycled Fine Aggregate Powder on Strength

After validating the developed ANN model (i.e., R^2 and MAE values were 0.92% and 1.68%, respectively), the model was used to evaluate the effect of incorporating different percentages of FRCP. Mixtures incorporating 20%, 30%, 35%, and 40% FRCP were introduced to the developed ANN model. The simulation results obtained for the recycled concrete compressive strength produced with different replacement levels of FRCP at curing days (7, 28, 60, 90, and 180 days) are displayed in Figure 6. In general, the compressive strength increased with time regardless of the amount of FRCP. Moreover, all tested mixtures exhibited compressive strengths above 32 MPa, which is the minimum decent concrete strength exposed to sulfate environment according to American Concrete Institute ACI Committee 318 [43]. One interesting point, the strength development rate differed as the FRCP amount exceeded 30%. Hence, similar to conventional concrete behavior, mixtures incorporating more than 30% FRCP exhibited slightly low early strength at seven days, while exhibiting high strength later at 180 days. For mixtures incorporating 20% FRCP, the compressive strengths at ages 7 and 180 days were 38.43 MPa and 46.31 MPa, respectively, indicating an increase of 28.3%. For mixtures incorporating 40% FRCP, the compressive strengths at ages 7 and 180 days were 34.29 MPa and 56.05 MPa, respectively, indicating an increase of 63.4%. It should be noted that an increase in the FRCP content considerably increased the gain of compressive strength for concrete at ages 7 days to 180 days. In summary, a compressive strength increase of 28.3% (strengths at age 7 days vs. 180 days) was reported for concrete with 20% FRCP, while a more significant increase of 63.4% (strengths at age 7 days vs. 180 days) was reported for concrete with 40% FRCP. Adding such fine materials was expected to modify the particle size distribution and, consequently, the initial porosity of the mixture. It was noticed that the more added fine materials, the denser the microstructure. However, increasing the fine materials was going to increase the surface area and, consequently, the amount of absorbed water, leaving less free water for hydration during the early period. At later ages, mixtures with a higher amount of fine materials will possess a lower number of voids that need to be filled by hydration products. Hence, any slight continuation in hydration will have a higher impact on strengthening the microstructure. Moreover, FRCP has old, hydrated cement, i.e., calcium hydroxide (C.H.). This highlights the potential of having a pozzolanic reaction that directly contributes to strength development through enhancing interfacial transition zone (ITZ), which is responsible for the higher bond between aggregate/cement paste [44,45]. Therefore, the higher the added FRCP, the more the C.H. and pozzolanic reaction leading to higher later strength.

3.3.2. Effect of Recycled Aggregate at Different FRAP Contents

The influence of recycled aggregate content was quantified for a concrete mixture with 350 kg cement and a water cement ratio W/C of 0.5. Three groups of mixtures were developed based on the FRCP content, which varied from 20% up to 35%. In each group, RCA content was varied from 0% up to 100% of the total aggregate as a replacement for natural aggregates. Regardless of RCA content, the compressive strength of recycled concrete increased as curing time increased (Figure 7a–c). Also, increasing the percentage of RCA resulted in higher compressive strength. For instance, for the group of mixtures with 20% FRCP at 28 days, replacing NA with 50% and 100% RCA resulted in 14.7% and 38% increase in the achieved strength. This strength development was due to concrete hardening and probably the strong bond between the recycled coarse aggregates and the cement paste in addition to the good quality of recycled aggregates used. This behavior was following the results observed by previous works [44–48].

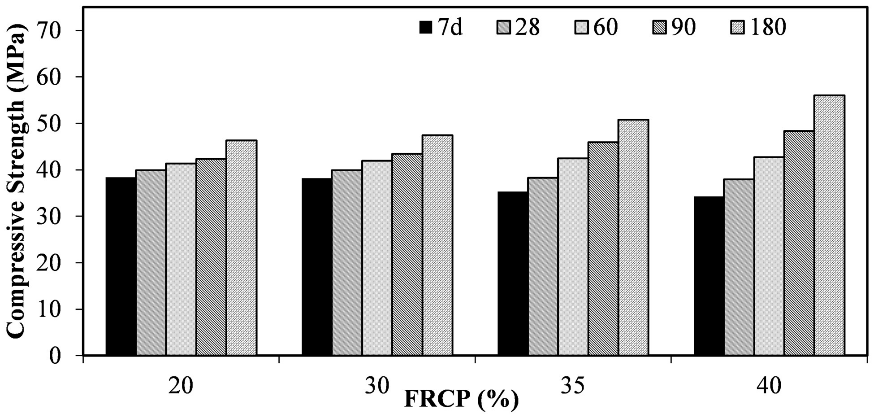

Figure 6. Simulation results of the RSCC compressive strength with 100% NA and different FRCP contents.

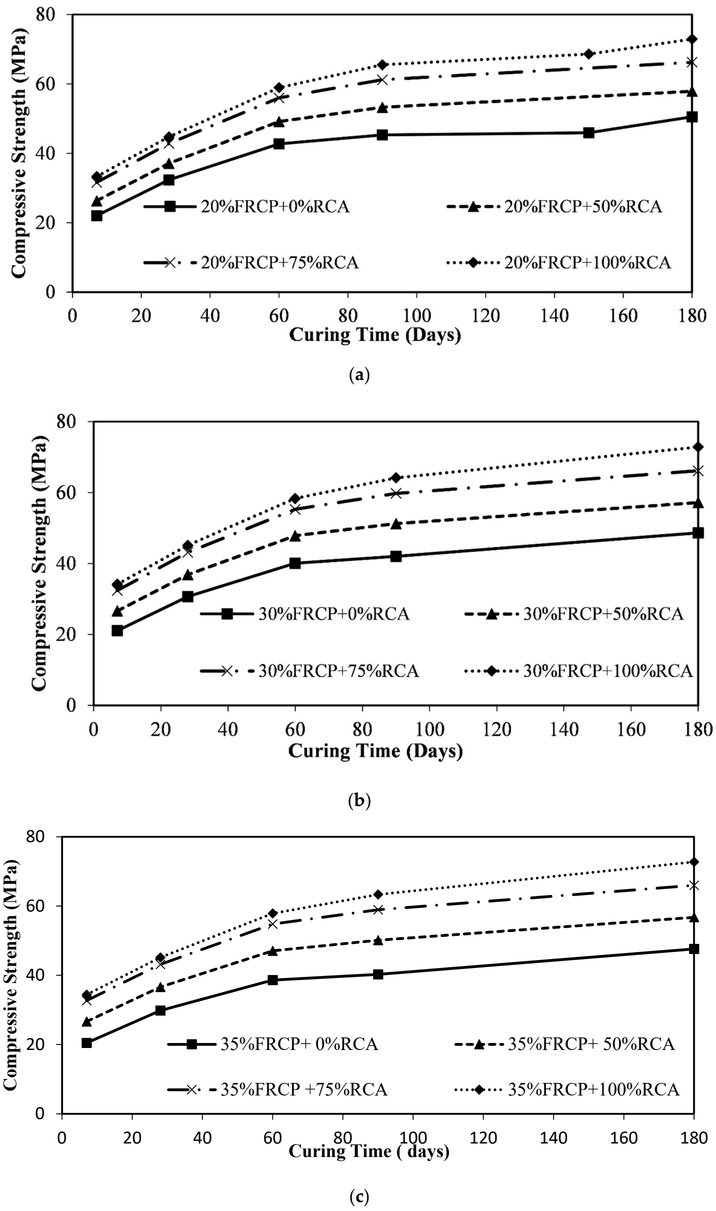

Figure 7. Simulation results of compressive strength of RSCC for different RCA contents (0–100%) and three contents of FRCP: (**a**) 20%, (**b**) 30%, and (**c**) 35%.

The combination of RCA and FRCP significantly affected the compressive strength of the concrete mixture. There were small differences in the percentage of reduction of the compressive strength between the experimental results and the predicted ones provided by the ANN model. The difference in compressive strength values was about 0.95% (less than 1%) for each age.

3.3.3. Combined Effect between FRAP and Fly Ash

Figure 8 shows the variations with the curing age of concrete compressive strengths for different contents of additives (fly ash contents and FRCP) at the same w/c ratio of 0.5.

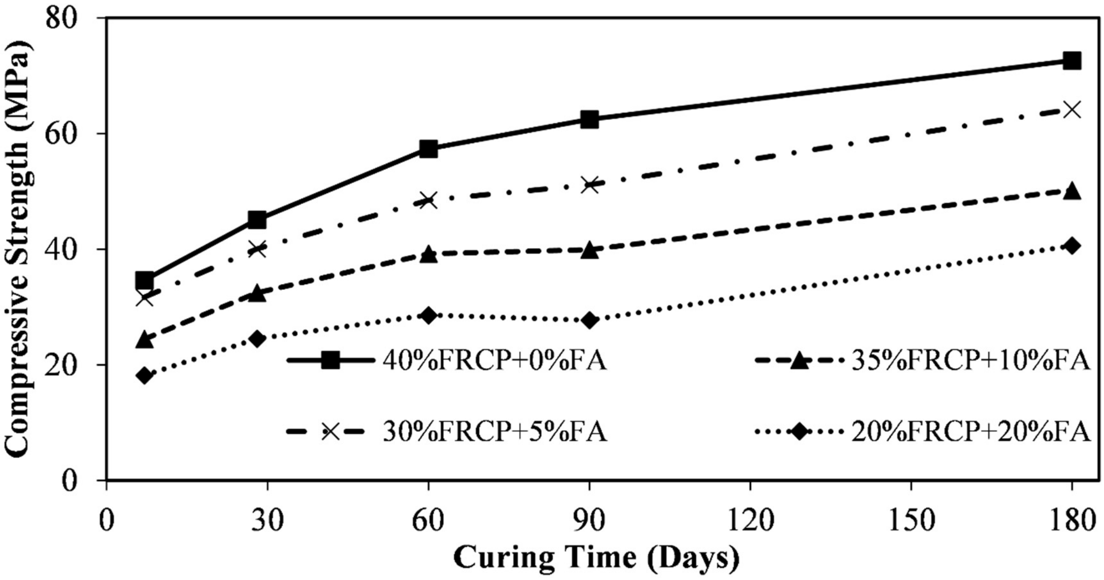

Figure 8. Simulation results of RSCC compressive strength produced from four combinations of FRCP and FA contents at different curing ages.

Generally, compressive strength increases with increasing curing age. For example, at 28 days, the compressive strength of concrete produced with 20 to 35% FRCP and 100% RCA remained above 32 MPa. Further, using fly ash as a partial replacement of cement caused a decrease in the compressive strength. Looking more closely at the simulated results for the strength development between the 28- and 180-day results shows that the mixtures prepared with 5, 10, and 20% fly ash exhibited reductions in the compressive strength of 11%, 28%, and 45.46% compared to the reference sample (i.e., 0% FA). On the other side, the combination of FRCP and fly ash significantly affected the compressive strength, as shown in Figure 8. In addition, the results from literature indicate that, with an increase in the FA content in recycled concrete produced with 100% RCA, the compressive strength decreases [26]. The existence of fly ash caused a decrease in the recycled concrete compressive strength, but the reductions were not critical in the long term (less than 11% at the curing age of 180 days) for the optimal mixture (100% RCA, 35% FRCP, and 10% FA). These results are consistent with previous findings showing that recycled aggregates (fine, powder) possess a particular self-cementing capacity [49].

Figure 9 depicts the influence of the fly ash percentage on the compressive strength of recycled concrete. As fly ash replacement level increased, the strength of concrete decreased. Using fly ash as a 5% substitution of ordinary cement and 40% FRCP substitution of natural pozzolanic influenced the strength. Its effect was marginal compared with 10, 15, and 20% FA. The presence of fly ash of less than 20% caused only a small decrease in the recycled concrete compressive strength compared to the conventional ones. A polynomial relationship between the additive contents (FRCP and/or FA) used and the compressive strength of RSCC was proposed to evaluate the properties over a wider set of curing days, more than 180 days (Figure 9).

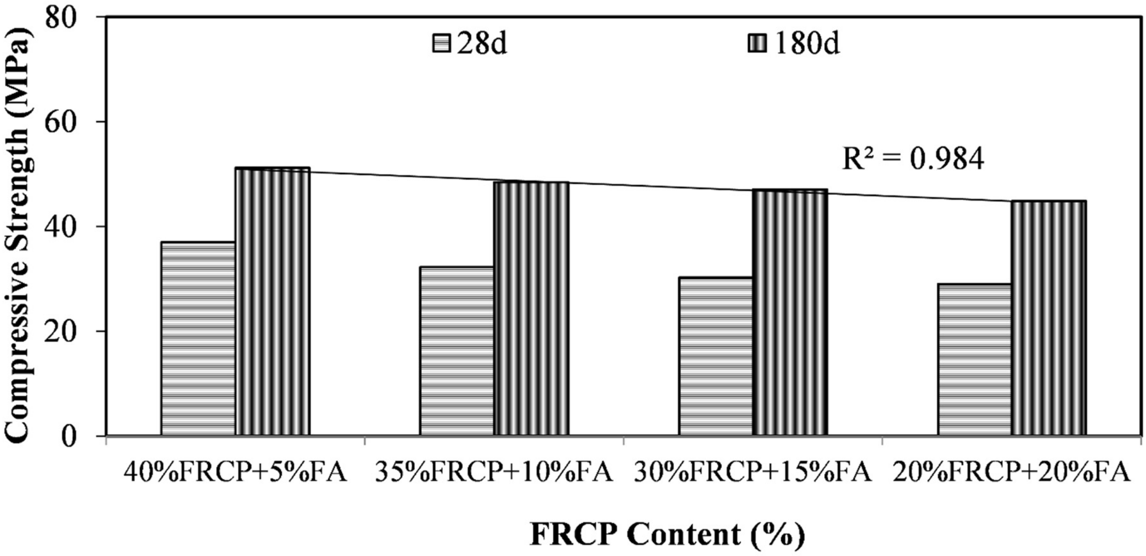

Figure 9. Simulation results of the effect of FRCP and FA contents on the strength of RSCC (100% RCA) after 28 and 180 curing days.

4. Conclusions

In the current study, the influence of fine, recycled concrete powder on the compressive strength of recycled self-compacting concrete was investigated using an artificial neural network. The main results may be summarized as follows:

- The proposed ANN model provided good accuracy for the prediction of the compressive strength of RSCC in the data used for training. The regression values obtained for the training, testing, and validation steps were entirely satisfactory, namely, 0.97, 0.96, and 0.96, respectively. The MSE of the model was 0.01. During the experimental validation, the regression value remained high (0.88). It can be expanded beyond the existing domain. Future experimental data are, however, required for such an extension.
- For validating the model, the actual experimental compressive strengths of RSCC were compared to the compressive strengths predicted by the model, showing a very good correlation (R^2- value of 0.88). Therefore, the results showed that the developed model can predict the compressive strength of RSCC with high accuracy.
- The type of aggregates, water absorption values, replacement level of RA and FRCP, and curing age can generally affect the properties of recycled concrete.
- The recycled self-compacting concrete compressive strength with any level of recycled aggregates can be significantly improved by using at least 40% of FRCP as cement replacement.
- The combination of fine, recycled concrete powder and recycled aggregates can have a positive effect on the mechanical properties of RSCC.

Incorporating fly ash ratio of less than 20% with recycled aggregates and fine, recycled aggregates did not show any significant effect on the compressive strength of RSCC.

Author Contributions: Conceptualization, S.B. and A.S.; methodology, S.B. and S.P., A.S.; software, S.B.; validation, S.B., and A.S.; formal analysis, S.B., B.A., A.H.R., S.P., and A.S.; investigation, S.B.; resources, S.P.; data curation, S.B.; writing—original draft preparation, S.B. and A.E.; writing—review and editing, S.P., and A.E.; visualization, S.B.; supervision, S.P., A.S.; project administration, S.B.; funding acquisition, S.B. All authors have read and agreed to the published version of the manuscript.

Funding: This research received no external funding.

Institutional Review Board Statement: Not applicable.

Informed Consent Statement: Not applicable.

Data Availability Statement: The data presented in this study are available on request from the corresponding author.

Acknowledgments: S.B. and S.P. would like to acknowledge the support of the NSERC chair on industrial energy efficiency established at Université de Sherbrooke in 2019 with the support of Hydro-Québec, Natural Resources Canada, and Emerson Canada.

Conflicts of Interest: The authors declare no conflict of interest. The funders had no role in the design of the study; in the collection, analyses, or interpretation of data; in the writing of the manuscript; or in the decision to publish the results.

Appendix A

Table A1. Details of the experimental database [3,26,44,49–59].

No (kg/m^3)	B (kg/m^3)	W/B	NA (kg/m^3)	NS (kg/m^3)	RS	RCA (kg/m^3)	FRCP (kg/m^3)	NP (kg/m^3)	FA (kg/m^3)	CT (days)	Sample Size (mm)	CS (MPa)	Shape Correction	CS of Cubes (MPa)	Normalized Strength *	Refs
1	449	0.35	898	898	0	0	0	0	0	7	(cylinder) 100 × 200	48.06	0.88	54.61	1.00	[50]
2	449	0.35	898	673	247.25	199	0	0	0	7		46.66	0.84	55.55	1.02	
3	449	0.35	898	449	494.5	379	0	0	0	7		38.19	0.78	48.96	0.90	
4	449	0.35	898	0	898	794	0	0	0	7		30.91	0.78	39.63	0.73	
5	449	0.35	898	673	247.25	203	0	0	0	7		47.53	0.84	56.58	1.04	
6	449	0.35	898	449	494.5	406	0	0	0	7		42.86	0.78	54.95	1.01	
7	449	0.35	898	822	898	813	0	0	0	7		41.12	0.78	52.72	0.97	
8	411	0.55	822	822	0	0	0	0	0	7		26.11	0.77	33.91	1.00	
9	411	0.55	822	616	102.75	182	0	0	0	7		22.03	0.76	28.99	0.85	
10	411	0.55	822	411	411	363	0	0	0	7		17.71	0.76	23.30	0.69	
11	411	0.55	822	0	411	727	0	0	0	7		12.75	0.76	16.78	0.49	
12	411	0.55	822	616	154	186	0	0	0	7		23.76	0.74	32.11	0.95	
13	411	0.55	822	411	205.5	372	0	0	0	7		22.77	0.74	30.77	0.91	
14	411	0.55	822	0	822	744	0	0	0	7		20.66	0.74	27.92	0.82	
15	449	0.35	898	898	0	0	0	0	0	14		53.12	0.88	60.36	1.00	
16	449	0.35	898	673	247.25	199	0	0	0	14		48.34	0.84	57.55	0.95	
17	449	0.35	898	449	494.5	379	0	0	0	14		41.97	0.78	53.81	0.89	
18	449	0.35	898	0	898	794	0	0	0	14		34.75	0.78	44.55	0.74	
19	449	0.35	898	673	247.25	203	0	0	0	14		49.64	0.84	59.10	0.98	
20	449	0.35	898	449	494.5	406	0	0	0	14		48.52	0.84	57.76	0.96	
21	449	0.35	898	822	898	813	0	0	0	14		46.73	0.84	55.63	0.92	
22	411	0.55	822	822	0	0	0	0	0	14		29	0.77	37.66	1.00	
23	411	0.55	822	616	102.75	182	0	0	0	14		24.72	0.74	33.41	0.89	

Table A1. *Cont.*

No (kg/m^3)	B (kg/m^3)	W/B	NA (kg/m^3)	NS (kg/m^3)	RS	RCA (kg/m^3)	FRCP (kg/m^3)	NP (kg/m^3)	FA (kg/m^3)	CT (days)	Sample Size (mm)	CS (MPa)	Shape Correction	CS of Cubes (MPa)	Normalized Strength *	Refs
24	411	0.55	822	411	411	363	0	0	0	14		21.51	0.74	29.07	0.77	
25	411	0.55	822	0	411	727	0	0	0	14		15.64	0.76	20.58	0.55	
26	411	0.55	822	616	154	186	0	0	0	14		26.71	0.74	36.09	0.96	
27	411	0.55	822	411	205.5	372	0	0	0	14		25.32	0.74	34.22	0.91	
28	411	0.55	822	0	822	744	0	0	0	14		23.78	0.74	32.14	0.85	
29	449	0.35	898	898	0	0	0	0	0	28		56.28	0.88	63.95	1.00	
30	449	0.35	898	673	247.25	199	0	0	0	28		51.44	0.84	61.24	0.96	
31	449	0.35	898	449	494.5	379	0	0	0	28		47.44	0.84	56.48	0.88	
32	449	0.35	898	0	898	794	0	0	0	28		37.77	0.78	48.42	0.76	
33	449	0.35	898	673	247.25	203	0	0	0	28		53.27	0.84	63.42	0.99	
34	449	0.35	898	449	494.5	406	0	0	0	28		51.34	0.84	61.12	0.96	
35	449	0.35	898	822	898	813	0	0	0	28		49.63	0.84	59.08	0.92	
36	411	0.55	822	822	0	0	0	0	0	28		34.1	0.82	41.59	1.00	
37	411	0.55	822	616	102.75	182	0	0	0	28		28.58	0.74	38.62	0.93	
38	411	0.55	822	411	411	363	0	0	0	28		24.6	0.74	33.24	0.80	
39	411	0.55	822	0	411	727	0	0	0	28		17.76	0.76	23.37	0.56	
40	411	0.55	822	616	154	186	0	0	0	28		31.31	0.78	40.14	0.97	
41	411	0.55	822	411	205.5	372	0	0	0	28		29.09	0.74	39.31	0.95	
42	411	0.55	822	0	822	744	0	0	0	28		27.26	0.74	36.84	0.89	
43	379	0.5	1171	379	0	0	0	0	0	7	(cube)100 × 100 × 100	26.2	1	26.2	1	[44]
44	379	0.5	0	379	0	1171	0	0	0	7		29.9	1	29.9	1.14	

Table A1. *Cont.*

No (kg/m³)	B (kg/m³)	W/B	NA (kg/m³)	NS (kg/m³)	RS	RCA (kg/m³)	FRCP (kg/m³)	NP (kg/m³)	FA (kg/m³)	CT (days)	Sample Size (mm)	CS (MPa)	Shape Correction	CS of Cubes (MPa)	Normalized Strength *	Refs
45	379	0.5	1171	379	0	0	0	0	0	28	(cube)100 × 100 × 100	32.6	1	32.6	1	[44]
46	379	0.5	0	379	0	1171	0	0	0	28		38.7	1	38.7	1.19	
47	379	0.5	1171	379	0	0	0	0	0	90	(cube)100 × 100 × 100	46.5	1	46.5	1	[44]
48	379	0.5	0	379	0	1171	0	0	0	90		55	1	55	1.18	
49	208	0.72	1040.7	807.6	0	0	0	0	52	7		12	0.84	14.29	1.00	
50	208	0.72	728.5	807.6	0	312.2	0	0	52	7		13.4	0.76	17.63	1.23	
51	208	0.72	624.4	807.6	0	416.3	0	0	52	7	(Cylinder) 100 × 200	9.6	0.76	12.63	0.88	[51]
52	208	0.72	520.4	807.6	0	520.4	0	0	52	7		10.1	0.76	13.29	0.93	
53	208	0.72	780.5	807.6	0	780.5	0	0	52	7		8.7	0.76	11.45	0.80	
54	208	0.72	1070.7	807.6	0	1040.7	0	0	52	7		8.9	0.76	11.71	0.82	
55	208	0.72	1040.7	807.6	0	0	0	0	52	28		17.1	0.81	21.11	1.00	
56	208	0.72	728.5	807.6	0	312.2	0	0	52	28		16.5	0.76	21.71	1.03	
57	208	0.72	624.4	807.6	0	416.3	0	0	52	28		16.3	0.76	21.45	1.02	
58	208	0.72	520.4	807.6	0	520.4	0	0	52	28		14.7	0.76	19.34	0.92	
59	208	0.72	780.5	807.6	0	780.5	0	0	52	28		15.1	0.76	19.87	0.94	
60	208	0.72	1070.7	807.6	0	1040.7	0	0	52	28		13.7	0.76	18.03	0.85	
61	208	0.72	1040.7	807.6	0	0	0	0	52	56		23	0.74	31.08	1.00	
62	208	0.72	728.5	807.6	0	312.2	0	0	52	56		22	0.76	28.95	0.93	
63	208	0.72	624.4	807.6	0	416.3	0	0	52	56		18	0.76	23.68	0.76	
64	208	0.72	520.4	807.6	0	520.4	0	0	52	56		18.9	0.76	24.87	0.80	
65	208	0.72	780.5	807.6	0	780.5	0	0	52	56		17.7	0.76	23.29	0.75	
66	208	0.72	1070.7	807.6	0	1040.7	0	0	52	56		16.6	0.76	21.84	0.70	
67	208	0.72	1040.7	807.6	0	0	0	0	52	148		24.1	0.77	31.30	1.00	
68	208	0.72	728.5	807.6	0	312.2	0	0	52	148		25.5	0.74	34.46	1.10	
69	208	0.72	624.4	807.6	0	416.3	0	0	52	148		19.9	0.76	26.18	0.84	

Table A1. *Cont.*

No (kg/m^3)	B (kg/m^3)	W/B	NA (kg/m^3)	NS (kg/m^3)	RS	RCA (kg/m^3)	FRCP (kg/m^3)	NP (kg/m^3)	FA (kg/m^3)	CT (days)	Sample Size (mm)	CS (MPa)	Shape Correction	CS of Cubes (MPa)	Normalized Strength *	Refs
70	208	0.72	520.4	807.6	0	520.4	0	0	52	148		19.8	0.76	26.05	0.83	
71	208	0.72	780.5	807.6	0	780.5	0	0	52	148		21	0.76	27.63	0.88	
72	208	0.72	1070.7	807.6	0	1040.7	0	0	52	148		20.6	0.76	27.11	0.87	
73	430	0.64	602	846	0	0	0	0	185	7	(Cube)100 × 100 × 100	26	1	26	1	[53]
74	430	0.64	301	846	0	278	0	0	185	7		23.5	1	23.5	0.90	
75	430	0.64	301	635	193	278	0	0	185	7		24	1	24	0.92	
76	430	0.64	301	423	386	278	0	0	185	7		24	1	24	0.92	
77	430	0.64	0	846	0	556	0	0	185	7		24	1	24	0.92	
78	430	0.64	0	556	193	556	0	0	185	7		25	1	25	0.96	
79	430	0.64	0	423	386	556	0	0	185	7		25	1	25	0.96	
80	430	0.64	602	846	0	0	0	0	185	28		37.5	1	37.5	1.00	
81	430	0.64	301	846	0	278	0	0	185	28		34	1	34	0.91	
82	430	0.64	301	635	193	278	0	0	185	28		35.5	1	35.5	0.95	
83	430	0.64	301	423	386	278	0	0	185	28		35	1	35	0.93	
84	430	0.64	0	846	0	556	0	0	185	28		36	1	36	0.96	
85	430	0.64	0	556	193	556	0	0	185	28		36.5	1	36.5	0.97	
86	430	0.64	0	423	386	556	0	0	185	28		35.5	1	35.5	0.95	
87	430	0.64	602	846	0	0	0	0	185	56		40	1	40	1.00	
88	430	0.64	301	846	0	278	0	0	185	56		35	1	35	0.88	
89	430	0.64	301	635	193	278	0	0	185	56		37	1	37	0.93	
90	430	0.64	301	423	386	278	0	0	185	56		36	1	36	0.90	
91	430	0.64	0	846	0	556	0	0	185	56		38	1	38	0.95	
92	430	0.64	0	556	193	556	0	0	185	56		39	1	39	0.98	
93	430	0.64	0	423	386	556	0	0	185	56		38	1	38	0.95	
94	430	0.64	602	846	0	0	0	0	185	120		47	1	47	1.00	

Table A1. *Cont.*

No (kg/m^3)	B (kg/m^3)	W/B	NA (kg/m^3)	NS (kg/m^3)	RS	RCA (kg/m^3)	FRCP (kg/m^3)	NP (kg/m^3)	FA (kg/m^3)	CT (days)	Sample Size (mm)	CS (MPa)	Shape Correction	CS of Cubes (MPa)	Normalized Strength *	Refs
95	430	0.64	301	846	0	278	0	0	185	120		41	1	41	0.87	
96	430	0.64	301	635	193	278	0	0	185	120		44	1	44	0.94	
97	430	0.64	301	423	386	278	0	0	185	120		42	1	42	0.89	
98	430	0.64	0	846	0	556	0	0	185	120		45	1	45	0.96	
99	430	0.64	0	556	193	556	0	0	185	120		47	1	47	1.00	
100	430	0.64	0	423	386	556	0	0	185	120		46	1	46	0.98	
101	310	0.4	1200	650	0	0	0	0	0	28		50	1	50	1.00	
102	310	0.4	920	650	0	140	0	0	0	28		49	1	49	0.98	
103	310	0.4	840	645	0	360	0	0	0	28	(Cube)100 × 100 × 100	49	1	49	0.98	[54]
104	310	0.4	590	640	0	590	0	0	0	28		45	1	45	0.90	
105	310	0.4	0	625	0	1170	0	0	0	28		42	1	42	0.84	
106	370	0.45	1215	650	0	0	0	0	0	7		19	1	19	1	
107	370	0.45	850.5	650	0	364.5	0	0	0	7		19	1	19	1	
108	370	0.45	607.5	650	0	607.5	0	0	0	7		19	1	19	1	
109	370	0.45	0	650	0	1215	0	0	0	7		19	1	19	1	
110	370	0.45	1215	650	0	0	0	0	0	28		41	1	41	1	
111	370	0.45	850.5	650	0	364.5	0	0	0	28	(Cube)100 × 100 × 100	40	1	40	0.98	[55]
112	370	0.45	607.5	650	0	607.5	0	0	0	28		41	1	41	1.00	
113	370	0.45	0	650	0	1215	0	0	0	28		40	1	40	0.98	
114	370	0.45	1215	650	0	0	0	0	0	90		64	1	64	1	
115	370	0.45	850.5	650	0	364.5	0	0	0	90		65	1	65	1.02	
116	370	0.45	607.5	650	0	607.5	0	0	0	90		64	1	64	1	
117	370	0.45	0	650	0	1215	0	0	0	90		65	1	65	1.02	

Table A1. *Cont.*

No (kg/m^3)	B (kg/m^3)	W/B	NA (kg/m^3)	NS (kg/m^3)	RS	RCA (kg/m^3)	FRCP (kg/m^3)	NP (kg/m^3)	FA (kg/m^3)	CT (days)	Sample Size (mm)	CS (MPa)	Shape Correction	CS of Cubes (MPa)	Normalized Strength *	Refs
118	400	0.48	1290	523	0	0	0	0	0	28	(cylinder) 160 × 300	42.6	0.78	54.62	1	[56]
119	400	0.43	1140	685	0	0	0	0	0	28		54.8	0.88	62.27	1	
120	400	0.5	0	787	0	824	0	0	0	28		43.3	0.82	52.80	1	
121	400	0.65	0	0	629	878	0	0	0	28		31.5	0.78	40.38	0.74	
122	400	0.6	0	0	659	746	0	0	0	28		35.4	0.78	45.38	0.83	
123	400	0.66	0	0	675	865	0	0	0	28		39.4	0.78	50.51	0.92	
124	360	0.65	1100	705	0	0	0	0	0	7	(Cube)100 × 100 × 100	17	1	17	1	[3]
125	360	0.65	0	705	0	1100	0	0	0	7		15	1	15	0.89	
126	380	0.5	1100	705	0	0	0	0	0	7		21.2	1	21.2	1	
127	380	0.5	0	705	0	1100	0	0	0	7		18.9	1	18.9	1.10	
128	400	0.48	1100	705	0	0	0	0	0	7		24.7	1	24.7	1	
129	400	0.48	0	705	0	1100	0	0	0	7		22.7	1	22.7	0.92	
130	420	0.43	1100	705	0	0	0	0	0	7		32.5	1	32.5	1	
131	420	0.43	0	705	0	1100	0	0	0	7		26.5	1	26.5	0.82	
132	460	0.4	1100	705	0	0	0	0	0	7		37.3	1	37.3	1	
133	460	0.4	0	705	0	1100	0	0	0	7		27.8	1	27.8	0.76	
134	360	0.65	1100	705	0	0	0	0	0	28		22.7	1	22.7	1	
135	360	0.65	0	705	0	1100	0	0	0	28		20.3	1	20.3	0.90	
136	380	0.5	1100	705	0	0	0	0	0	28		32.3	1	32.3	1.00	
137	380	0.5	0	705	0	1100	0	0	0	28		29.2	1	29.2	0.91	
138	400	0.48	1100	705	0	0	0	0	0	28		36	1	36	1	
139	400	0.48	0	705	0	1100	0	0	0	28		32.2	1	32.3	0.90	
140	420	0.43	1100	705	0	0	0	0	0	28		46	1	46	1	

Table A1. *Cont.*

No (kg/m^3)	B (kg/m^3)	W/B	NA (kg/m^3)	NS (kg/m^3)	RS	RCA (kg/m^3)	FRCP (kg/m^3)	NP (kg/m^3)	FA (kg/m^3)	CT (days)	Sample Size (mm)	CS (MPa)	Shape Correction	CS of Cubes (MPa)	Normalized Strength *	Refs
141	420	0.43	0	705	0	1100	0	0	0	28		39.4	1	39.4	0.86	
142	460	0.4	1100	705	0	0	0	0	0	28		53.5	1	53.5	1.34	
143	460	0.4	0	705	0	1100	0	0	0	28		46.5	1	46.5	0.87	
144	325	0.5	1206.4	710.5	0	0	0	0	0	7	(Cube)100 × 100 × 100	50	1	50	1.00	[57]
145	325	0.5	0	660.7	0	1106.8	0	0	0	7		40	1	40	0.81	
146	345	0.43	0	613.9	0	1109.4	0	0	0	7		45	1	45	0.90	
147	365	0.4	0	586.8	0	1126.8	0	0	0	7		50	1	50	1	
148	365	0.4	0	586.5	0	1126.8	0	0	0	7		50	1	50	1	
149	325	0.5	0	660	0	1106.8	0	0	0	7		35	1	35	0.71	
150	325	0.5	1206.4	710.5	0	0	0	0	0	28		60	1	60	1.00	
151	325	0.5	0	660.7	0	1106.8	0	0	0	28		45	1	45	0.76	
152	345	0.43	0	613.9	0	1109.4	0	0	0	28		51	1	51	0.85	
153	365	0.4	0	586.8	0	1126.8	0	0	0	28		55	1	55	0.92	
154	365	0.4	0	586.5	0	1126.8	0	0	0	28		55	1	55	0.92	
155	325	0.5	0	660	0	1106.8	0	0	0	28		40	1	40	0.68	
156	250	0.6	1188	795	0	0	0	0	0	7	(Cylinder) 100 × 200	35.9	0.82	43.78	1.00	[58]
157	250	0.6	0	795	0	1021	0	0	0	7		30	0.74	40.54	0.93	
158	350	0.45	1148	696	0	0	0	0	0	7		53.6	0.88	60.91	1.00	
159	350	0.45	0	696	0	1016	0	0	0	7		43.8	0.82	53.41	0.88	
160	450	0.35	1170	596	0	0	0	0	0	7		66.6	0.88	75.68	1.00	
161	450	0.35	0	596	0	1027	0	0	0	7		52.7	0.84	62.74	0.83	
162	350.25	0.45	861	696	0	254	0	0	0	7		52	0.84	61.90	1.02	
163	350.5	0.45	574	696	0	507	0	0	0	7		49.4	0.84	58.81	0.97	
164	250	0.6	1188	795	0	0	0	0	0	28		43.5	0.82	53.05	1.00	

Table A1. *Cont.*

No (kg/m^3)	B (kg/m^3)	W/B	NA (kg/m^3)	NS (kg/m^3)	RS	RCA (kg/m^3)	FRCP (kg/m^3)	NP (kg/m^3)	FA (kg/m^3)	CT (days)	Sample Size (mm)	CS (MPa)	Shape Correction	CS of Cubes (MPa)	Normalized Strength *	Refs
165	250	0.6	0	795	0	1021	0	0	0	28		38.2	0.82	46.59	0.88	
166	350	0.45	1148	696	0	0	0	0	0	28		61.7	0.88	70.11	1.00	
167	350	0.45	0	696	0	1016	0	0	0	28		52.8	0.84	62.86	0.90	
168	450	0.35	1170	596	0	0	0	0	0	28		74.4	0.88	84.55	1.00	
169	450	0.35	0	596	0	1027	0	0	0	28		62.8	0.84	74.76	0.88	
170	350.25	0.45	861	696	0	254	0	0	0	28		60.7	0.84	72.26	1.00	
171	350.5	0.45	574	696	0	507	0	0	0	28		59.4	0.84	70.71	1.01	
172	350	0.5	791	627.81	0	0	0	140	0	7	(Cube) 70 × 70 × 70	25	0.97	24.25	1.00	[26]
173	350	0.5	0	627.81	0	791	0	140	0	7		27	0.97	26.19	1.08	
174	350	0.5	791	627.81	0	0	140	0	0	7		28	0.97	27.16	1.12	
175	350	0.5	0	627.81	0	791	140	0	0	7		26	0.97	25.22	1.04	
176	350	0.5	791	627.81	0	0	0	140	0	28		40.33	0.97	39.12	1.00	
177	350	0.5	0	627.81	0	791	0	140	0	28		39.33	0.97	38.15	0.98	
178	350	0.5	791	627.81	0	0	140	0	0	28		45.67	0.97	44.3	1.13	
179	350	0.5	0	627.81	0	791	140	0	0	28		44	0.97	42.68	1.09	
180	350	0.5	791	627.81	0	0	0	140	0	90		46.83	0.97	45.43	1.00	
181	350	0.5	0	627.81	0	791	0	140	0	90		47.67	0.97	46.24	1.02	
182	350	0.5	791	627.81	0	0	0	140	0	28		38	0.97	36.86	1.00	
183	350	0.5	0	627.81	0	791	0	140	0	28		40	0.97	38.8	1.05	
184	350	0.5	791	627.81	0	0	140	0	0	28		37	0.97	35.89	0.97	
185	350	0.5	0	627.81	0	791	140	0	0	28		42	0.97	40.74	1.11	
186	350	0.5	791	627.81	0	0	0	140	0	90		43	0.97	41.71	1.00	
187	350	0.5	0	627.81	0	791	0	140	0	90		45	0.97	43.65	1.05	
188	350	0.5	791	627.81	0	0	140	0	0	90		58	0.97	56.26	1.35	

Table A1. *Cont.*

No (kg/m^3)	B (kg/m^3)	W/B	NA (kg/m^3)	NS (kg/m^3)	RS	RCA (kg/m^3)	FRCP (kg/m^3)	NP (kg/m^3)	FA (kg/m^3)	CT (days)	Sample Size (mm)	CS (MPa)	Shape Correction	CS of Cubes (MPa)	Normalized Strength *	Refs
189	350	0.5	0	627.81	0	791	140	0	0	90		48	0.97	46.56	1.12	
190	350	0.5	791	627.81	0	0	0	140	0	180		48	0.97	46.56	1.00	
191	350	0.5	0	627.81	0	791	0	140	0	180		50.5	0.97	48.99	1.05	
192	350	0.5	791	627.81	0	0	140	0	0	180		60.17	0.97	58.36	1.25	
193	350	0.5	0	627.81	0	791	140	0	0	180		52	0.97	50.44	1.08	
194	325	0.5	0	710.5	0	1206.5	0	0	0	7		49.5	0.84	58.93	1.00	
195	325	0.2	0	660.7	0	1106.8	0	0	0	7		40.5	0.78	51.92	0.88	
196	345	0.43	0	613.9	0	1109.4	0	0	0	7		45.4	0.84	54.05	0.92	
197	365	0.4	0	586.8	0	1126.8	0	0	0	7		49	0.84	58.33	0.99	
198	365	0.4	0	586.8	0	1126.8	0	0	0	7		49.5	0.84	58.93	1.00	
199	325	0.52	0	660.7	0	1106.8	0	0	0	7		34.7	0.78	44.49	0.75	
200	325	0.5	0	710.5	0	1206.5	0	0	0	28		60.3	0.88	68.52	1.16	
201	325	0.2	0	660.7	0	1106.8	0	0	0	28		46.5	0.84	55.36	0.94	
202	345	0.43	0	613.9	0	1109.4	0	0	0	28		51.3	0.84	61.07	1.04	
203	365	0.4	0	586.8	0	1126.8	0	0	0	28	(cylinder) 100 × 200	56.1	0.84	66.79	1.13	[49]
204	365	0.4	0	586.8	0	1126.8	0	0	0	28		55.6	0.84	66.19	1.12	
205	325	0.52	0	660.7	0	1106.8	0	0	0	28		40.3	0.78	51.67	0.88	
206	300	0.55	1206.97	765.13	0	0	0	0	0	7		37.13	0.82	45.28	1.00	
207	300	0.55	787.4	765.1	0	1042.6	0	0	0	7		40.5	0.78	51.92	1.1	
208	318	0.52	1145.3	739	0	888.7	0	0	0	7		37.5	0.78	48.08	1.1	
209	325	0.5	1806.6	683.2	0	1123.4	0	0	0	7		40.4	0.78	51.79	1.1	
210	300	0.55	1206.97	765.13	0	0	0	0	0	28		44.3	0.82	54.02	1	
211	300	0.55	787.4	765.1	0	1042.6	0	0	0	28		46	0.84	54.76	1.01	
212	318	0.52	1145.3	739	0	888.7	0	0	0	28		43	0.78	55.13	1.01	

Table A1. *Cont.*

No (kg/m^3)	B (kg/m^3)	W/B	NA (kg/m^3)	NS (kg/m^3)	RS	RCA (kg/m^3)	FRCP (kg/m^3)	NP (kg/m^3)	FA (kg/m^3)	CT (days)	Sample Size (mm)	CS (MPa)	Shape Correction	CS of Cubes (MPa)	Normalized Strength *	Refs
213	325	0.5	1806.6	683.2	0	1123.4	0	0	0	28		46.13	0.84	54.92	1.02	
214	282.8	0.41	1050.5	757.6	0	0	0	0	70.7	3	(cylinder) 100 × 200	22.7	0.74	30.68	1.00	[52]
215	280	0.41	322.5	750	0	728	0	0	70	3		21.8	0.82	26.59	0.87	
216	277.2	0.41	432.7	742.6	0	617.8	0	0	69.3	3		21.7	0.82	26.46	0.86	
217	277.2	0.41	535.6	742.6	0	514.9	0	0	69.3	3		17.6	0.76	23.16	0.75	
218	282.8	0.41	1050.5	757.6	0	0	0	0	70.7	7		27.5	0.77	35.71	1.00	
219	280	0.41	322.5	750	0	728	0	0	70	7		26.8	0.74	36.22	1.01	
220	277.2	0.41	432.7	742.6	0	617.8	0	0	69.3	7		28.2	0.74	38.11	1.07	
221	277.2	0.41	535.6	742.6	0	514.9	0	0	69.3	7		24.9	0.74	33.65	0.94	
222	282.8	0.41	1050.5	757.6	0	0	0	0	70.7	28		35.5	0.82	43.29	1.00	
223	280	0.41	322.5	750	0	728	0	0	70	28		35.6	0.78	45.64	1.05	
224	277.2	0.41	432.7	742.6	0	617.8	0	0	69.3	28		33.1	0.78	42.44	0.98	
225	277.2	0.41	535.6	742.6	0	514.9	0	0	69.3	28		30.4	0.78	38.97	0.9	
226	282.8	0.41	1050.5	757.6	0	0	0	0	70.7	56		36.8	0.82	44.88	1.00	
227	280	0.41	322.5	750	0	728	0	0	70	56		37.2	0.78	47.69	1.06	
228	277.2	0.41	432.7	742.6	0	617.8	0	0	69.3	56		35.3	0.78	45.26	1.00	
229	277.2	0.41	535.6	742.6	0	514.9	0	0	69.3	56		35.9	0.78	46.03	1.02	
230	282.8	0.41	1050.5	757.6	0	0	0	0	70.7	120		49.8	0.88	56.59	1.00	
231	280	0.41	322.5	750	0	728	0	0	70	120		48.1	0.84	57.26	1.01	
232	277.2	0.41	432.7	742.6	0	617.8	0	0	69.3	120		47.6	0.84	56.67	1.00	
233	277.2	0.41	535.6	742.6	0	514.9	0	0	69.3	120		43.8	0.78	56.15	0.99	

Table A1. *Cont.*

No (kg/m^3)	B (kg/m^3)	W/B	NA (kg/m^3)	NS (kg/m^3)	RS	RCA (kg/m^3)	FRCP (kg/m^3)	NP (kg/m^3)	FA (kg/m^3)	CT (days)	Sample Size (mm)	CS (MPa)	Shape Correction	CS of Cubes (MPa)	Normalized Strength *	Refs
234	350	0.53	860	1050	0	0	0	0	0	28	(Cube)100 × 100 × 100	44.1	1	44.1	1.00	[59]
235	350	0.53	860	946	105	0	0	0	0	28		43	1	43	0.98	
236	350	0.53	860	840	210	0	0	0	0	28		42	1	42	0.95	
237	350	0.53	860	735	315	0	0	0	0	28		39	1	39	0.88	
238	350	0.53	860	630	420	0	0	0	0	28		35	1	35	0.79	
239	350	0.53	860	525	525	0	0	0	0	28		36	1	36	0.82	
240	350	0.53	860	0	1050	0	0	0	0	28		28.5	1	28.5	0.65	

B: binder. W/B: water-binder ratio. NA: natural aggregate. NS: natural sand. RS: recycled sand. RCA: recycled concrete aggregate. FRCP: fine recycled concrete powder. NP: natural pouzolana. FA: fly ash. CT: curing time. CS: compressive strength. Shape correction: shape conversion factor the cylindrical samples to cubic. * These values were normalized based on the 28 days strength for mixtures without recycled aggregate.

References

1. Kou, S.C.; Poon, C.S.; Chan, D. Influence of fly ash as a cement addition on the hardened properties of recycled aggregate concrete. *Mater. Struct.* **2007**, *41*, 1191–1201. [CrossRef]
2. Huseien, G.F.; Shah, K.W. Durability and life cycle evaluation of self-compacting concrete containing fly ash as GBFS replacement with alkali activation. *Constr. Build. Mater.* **2020**, *235*, 117458. [CrossRef]
3. Rahal, K. Mechanical properties of concrete with recycled coarse aggregate. *Build. Environ.* **2007**, *42*, 407–415. [CrossRef]
4. Chakkamalayath, J.; Joseph, A.; Al-Baghli, H.; Hamadah, O.; Dashti, D.; Abdulmalek, N. Performance evaluation of self-compacting concrete containing volcanic ash and recycled coarse aggregates. *Asian J. Civ. Eng.* **2020**, *21*, 815–827. [CrossRef]
5. Sonebi, M. Medium strength self-compacting concrete containing fly ash: Modelling using factorial experimental plans. *Cem. Concr. Res.* **2004**, *34*, 1199–1208. [CrossRef]
6. Panda, K.; Bal, P. Properties of Self Compacting Concrete Using Recycled Coarse Aggregate. *Procedia Eng.* **2013**, *51*, 159–164. [CrossRef]
7. Wang, Y.L.; Wang, W.D.; Guan, X.M. Physical Filling Effects of Limestone Powders with Different Particle Size. *Adv. Mater. Res.* **2010**, *163-167*, 1419–1424. [CrossRef]
8. Safiuddin, M.D.; Salam, M.A.; Jumaat, M.Z. Effects of recycled concrete aggregate on the fresh properties of self-consolidating concrete. *Arch. Civ. Mech. Eng.* **2011**, *11*, 1023–1041. [CrossRef]
9. Kou, S.; Poon, C. Properties of self-compacting concrete prepared with coarse and fine recycled concrete aggregates. *Cem. Concr. Compos.* **2009**, *31*, 622–627. [CrossRef]
10. Sasanipour, H.; Aslani, F. Durability properties evaluation of self-compacting concrete prepared with waste fine and coarse recycled concrete aggregates. *Constr. Build. Mater.* **2020**, *236*, 117540. [CrossRef]
11. González-Taboada, I.; González-Fonteboa, B.; Martínez-Abella, F.; Pérez-Ordóñez, J.L. Prediction of the mechanical properties of structural recycled concrete using multivariable regression and genetic programming. *Constr. Build. Mater.* **2016**, *106*, 480–499. [CrossRef]
12. Younis, K.H.; Pilakoutas, K. Strength prediction model and methods for improving recycled aggregate concrete. *Constr. Build. Mater.* **2013**, *49*, 688–701. [CrossRef]
13. Féret, R. Sur la compacité des matériaux hydrauliques. *Ann. Ponts Chaussées.* **1982**, *4*, 5–164.
14. Yang, J.; Du, Q.; Bao, Y. Concrete with recycled concrete aggregate and crushed clay bricks. *Constr. Build. Mater.* **2011**, *25*, 1935–1945. [CrossRef]
15. Rebouh, R.; Boukhatem, B.; Ghrici, M.; Tagnit-Hamou, A. A practical hybrid NNGA system for predicting the compressive strength of concrete containing natural pozzolan using an evolutionary structure. *Constr. Build. Mater.* **2017**, *149*, 778–789. [CrossRef]
16. Ni, H.-G.; Wang, J.-Z. Prediction of compressive strength of concrete by neural networks. *Cem. Concr. Res.* **2000**, *30*, 1245–1250. [CrossRef]
17. Duan, Z.; Kou, S.; Poon, C. Prediction of compressive strength of recycled aggregate concrete using artificial neural networks. *Constr. Build. Mater.* **2013**, *40*, 1200–1206. [CrossRef]
18. Topçu, İ.B.; Sarıdemir, M. Prediction of properties of waste AAC aggregate concrete using artificial neural network. *Comput. Mater. Sci.* **2007**, *41*, 117–125. [CrossRef]
19. Kasperkiewicz, J.; Racz, J.; Dubrawski, A. HPC Strength Prediction Using Artificial Neural Network. *J. Comput. Civ. Eng.* **1995**, *9*, 279–284. [CrossRef]
20. Yeh, I.-C. Design of High-Performance Concrete Mixture Using Neural Networks and Nonlinear Programming. *J. Comput. Civ. Eng.* **1999**, *13*, 36–42. [CrossRef]
21. Uysal, M.; Tanyildizi, H. Predicting the core compressive strength of self-compacting concrete (SCC) mixtures with mineral additives using artificial neural network. *Constr. Build. Mater.* **2011**, *25*, 4105–4111. [CrossRef]
22. Fan, C.-C.; Huang, R.; Hwang, H.; Chao, S.-J. The Effects of Different Fine Recycled Concrete Aggregates on the Properties of Mortar. *Materials* **2015**, *8*, 2658–2672. [CrossRef]
23. Zhou, C.; Chen, Z. Mechanical properties of recycled concrete made with different types of coarse aggregate. *Constr. Build. Mater.* **2017**, *134*, 497–506. [CrossRef]
24. Lee, B.Y.; Kim, J.H.; Kim, J.-K. Optimum concrete mixture proportion based on a database considering regional characteristics. *J. Comput. Civ. Eng.* **2009**, *23*, 258–265. [CrossRef]
25. Transportation Research Circulars. *Use of Artificial Neural Networks in Geomechanical and Pavement Systems*; Number E-C012; Transportation Research Board, National Research Council: Washington, DC, USA, 1999.
26. Boudali, S.; Kerdal, D.; Ayed, K.; Abdulsalam, B.; Soliman, A. Performance of self-compacting concrete incorporating recycled concrete fines and aggregate exposed to sulphate attack. *Constr. Build. Mater.* **2016**, *124*, 705–713. [CrossRef]
27. Haykin, S. *Neural Networks: A Comprehensive Foundation*; Prentice Hall: Upper Saddle River, NJ, USA, 1999.
28. Trabelsi, S.; Hafid, M.; Poncet, S.; Poirier, M.; Lacroix, M. Rheology of ethylene- and propylene-glycol ice slurries: Experiments and ANN model. *Int. J. Refrig.* **2017**, *82*, 447–460. [CrossRef]
29. Samui, P.; Das, S.D.; Sitharam, T.G. *Intelligent and Soft Computing in Infrastructure Systems Engineering*; Intel. & Soft Comp. in Infra. Sys. Eng., SCI 259; Gopalakrishnan, K., Ceylan, H., Attoh-Okine, N.O., Eds.; Springer: Berlin, Germany, 2009; pp. 305–323.
30. Sarıdemir, M. Predicting the compressive strength of mortars containing metakaolin by artificial neural networks and fuzzy logic. *Adv. Eng. Softw.* **2009**, *40*, 920–927. [CrossRef]
31. Nehdi, M.L.; Soliman, A.M. Artificial Intelligence Model for Early-Age Autogenous Shrinkage of Concrete. *ACI Mater. J.* **2012**, *109*, 353–361.

32. Nehdi, M.L.; El Chabib, H.; El Naggar, M.H. Predicting Performance of Self-Compacting Concrete Mixtures Using Artificial Neural Networks. *Mater. J.* **2001**, *98*, 394–401.
33. Comité Européen de Normalisation (CEN). *EN-1992-1-1: Eurocode 2: Design of Concrete Structures: Part 1-1: General Rules and Rules for Buildings*; Comité Européen de Normalisation (CEN): Brussels, Belgium, 2008; p. 259.
34. João Nuno, P.; de Jorge, B.; Carlos, C.; Luís, E. Probabilistic Conversion of the Compressive Strength of Cubes to Cylinders of Natural and Recycled Aggregate Concrete Specimens. *Mater. J.* **2009**, *12*, 1–11.
35. Zain, M.F.M.; Abd, S.M. Multiple Regression Model for Compressive Strength Prediction of High Performance Concrete. *J. Appl. Sci.* **2008**, *9*, 155–160. [CrossRef]
36. Demuth, H.; Beale, M. *Neural Network Toolbox 5, User's Guide*; MathWorks Inc.: Natick, MA, USA, 2007.
37. Smith, G.N. *Probability and Statistics in Civil Engineering: An Introduction*; Collins: London, UK, 1986.
38. Boudali, S.; Abdulsalam, B.; Soliman, A.M.; Ayed, K.; Kerdal, D.E. *Green Self-Compacting Sand Concrete Exposed to Sulfate Attack*; CSCE Resilient Infrastructure: London, UK, 2016; pp. 1–11.
39. DIN Standards Committee Building and Civil Engineering, European Standard Norme EN. *Cement—Part 1: Composition, Specifications and Conformity Criteria for Common Cements 197-1*; European Committee for Standardization: Brussels, Belgium, 2000; pp. 1–29.
40. American Society for Testing and Materials (ASTM) C494. *Standard Specification for Chemical Admixtures for Concrete*; American Society for Testing and Materials (ASTM): West Conshohocken, PA, USA, 2015.
41. ASTM C192. *Standard Practice for Making and Curing Concrete Test Specimens in the Laboratory*; American Society for Testing and Materials: West Conshohocken, PA, USA, 2012.
42. *NF P 18-400 Concretes—Moulds for Cylindrical and Prismatic Test*; Association Française de NORmalisation AFNOR: Paris, France, 1981; ISBN 978-2-12-131871-4.
43. ACI Committee 318. *Building Code Requirements for Structural Concrete and Commentary*; American Concrete Institute: Farmington Hills, MI, USA, 2014; p. 520.
44. Poon, C.; Shui, Z.; Lam, L. Effect of microstructure of ITZ on compressive strength of concrete prepared with recycled aggregates. *Constr. Build. Mater.* **2004**, *18*, 461–468. [CrossRef]
45. Boudali, S.; Soliman, A.M.; Abdulsalam, B.; Ayed, K.; Kerdal, D.E.; Poncet, S. Microstructural Properties of the Interfacial Transition Zone and Strength Development of Concrete Incorporating Recycled Concrete Aggregate. *Int. J. Civil Envir. Struct. Constr. Archit. Eng.* **2017**, *11*, 966–970.
46. Señas, L.; Priano, C.; Marfil, S. Influence of recycled aggregates on properties of self-consolidating concretes. *Constr. Build. Mater.* **2016**, *113*, 498–505. [CrossRef]
47. Gayarre, F.L.; Serna, P.; Cabo, A.D.; López, M.; Ángel, S.; López-Colina, C. Influence of recycled aggregate quality and proportioning criteria on recycled concrete properties. *Waste Manag.* **2009**, *29*, 3022–3028. [CrossRef] [PubMed]
48. Sim, J.; Park, C. Compressive strength and resistance to chloride ion penetration and carbonation of recycled aggregate concrete with varying amount of fly ash and fine recycled aggregate. *Waste Manag.* **2011**, *31*, 2352–2360. [CrossRef]
49. Yaprak, H.; Aruntas, H.Y.; Demir, I.; Simsek, O. Effects of the fine recycled concrete aggregates on the concrete properties. *Int. J. Phys. Sci.* **2011**, *6*, 2455–2461.
50. Fan, C.-C.; Huang, R.; Hwang, H.; Chao, S.-J. Properties of concrete incorporating fine recycled aggregates from crushed concrete wastes. *Constr. Build. Mater.* **2016**, *112*, 708–715. [CrossRef]
51. Huda, S.B. Mechanical and Durability Properties of Recycled and Repeated Recycled Coarse Aggregate Concrete. Ph.D. Thesis, University of Britsh Columbia, Vancouver, BC, Canada, 2014.
52. Huda, S.B.; Alam, M.S. Mechanical and Freeze-Thaw Durability Properties of Recycled Aggregate Concrete Made with Recycled Coarse Aggregate. *J. Mater. Civ. Eng.* **2015**, *27*, 04015003. [CrossRef]
53. Kapoor, K.; Singh, S.P.; Singh, B. Water Permeation Properties of Self Compacting Concrete Made with Coarse and Fine Recycled Concrete Aggregates. *Int. J. Civ. Eng.* **2016**, *16*, 47–56. [CrossRef]
54. Corinaldesi, V. Mechanical and elastic behaviour of concretes made of recycled-concrete coarse aggregates. *Constr. Build. Mater.* **2010**, *24*, 1616–1620. [CrossRef]
55. Limbachiya, M.C.; Leelawat, T.; Dhir, R.K. Use of recycled concrete aggregate in high-strength concrete. *Mater. Struct.* **2000**, *33*, 574–580. [CrossRef]
56. Buyle-Bodin, F.; Hadjieva-Zaharieva, R. Influence of industrially produced recycled aggregates on flow properties of concrete. *Mater. Struct.* **2002**, *35*, 504–509. [CrossRef]
57. Etxeberria, M.; Vázquez, E.; Marí, A.; Barra, M. Influence of amount of recycled coarse aggregates and production process on properties of recycled aggregate concrete. *Cem. Concr. Res.* **2007**, *37*, 735–742. [CrossRef]
58. Corinaldesi, V.; Moriconi, G. The role of industrial by-products in self-compacting concrete. *Constr. Build. Mater.* **2011**, *25*, 3181–3186. [CrossRef]
59. Etxeberria Larrañaga, M. Experimental Study on Microstructure and Structural Behaviour of Recycled Aggregate Concrete. Ph.D. Thesis, Universitat Politecnica de Catalunya, Barcelona, Spain, 2004.